Article

Mitigation Effect of Seismic Acceleration of Nuclear Power Plant Electric Cabinet Using Tuned Mass Damper under Earthquakes

Seongkyu Chang [1,*] and Sung Gook Cho [2]

[1] Academic-Industry Cooperation Foundation, Kunsan National University, Jeonbuk, Republic of Korea; s9752033@gmail.com
[2] R&D center, Innose Tech Co. Ltd., Incheon 406-840, Republic of Korea; sgcho@innosetech.com
* Correspondence: s9752033@gmail.com; Tel.: +82-(0)10-2758-7547

Abstract: In this study, a tuned mass damper is proposed as a seismic acceleration mitigating technique of an electrical cabinet inside the nuclear power plant. In order to know the mitigation performance, the electrical cabinet and the tuned mass damper were modeled using SAP2000. The sine sweep wave was used to confirm the vibration characteristics of the cabinet over a wide frequency range, and the several various earthquakes were applied to the cabinet to verify the control performance of the tuned mass damper. After analyzing the numerical results, it is summarized that the application of the proposed technique can reduce the acceleration response of the cabinet.

Keywords: nuclear power plant; electric cabinet; tuned mass damper; earthquake; vibration control

---

1. Introduction

Containment of nuclear power plants (NPP) occupies a very important place in terms of their necessity and safety requirements. This is because of the large ripple effect when damaged by the external force (earthquake, etc.). Therefore, the containment of NPPs needs careful attention from the design stage and its safety should be reviewed during operation. To fulfill these requirements, the containment of NPPs is carried out in seismic design with the highest safety allowance compared to other structures.

Nevertheless, if the equipment inside the containment is damaged during an earthquake, it can affect the core and, as a result, may cause fatal harm to the containment. Many electrical control devices are installed and operated at NPPs cabinet type equipment. Before installing the cabinet in the field, it should be seismically qualified at such level, that it can maintain its performance in vibrations in the design earthquake level.

As because of the recently happened earthquakes in Korea, whose magnitudes are more than 5.0, the seismic demand performance for internal equipment of NPPs is increasing. As a result, seismic reinforcement is required for the devices that do not satisfy the seismic demand performance in existing internal NPPs.

The seismic reinforcement method to improve the seismic performance of the internal electrical cabinet of NPPs includes a seismic restraint method, seismic isolation system and vibration control device. The seismic restraint method fixes the bottom or top of the cabinet using strut bolts or external angle brackets [1].

As a seismic isolation method, the seismic force from the floor is prevented from being transmitted to the upper structure, such as a friction pendulum system (FPS). Kim et al. [2] attempted to introduce the FPS to improve the seismic performance of the main control room of NPP and showed that the acceleration of the superstructure was reduced through the shaking table test. Kim

Preprints (www.preprints.org) | NOT PEER-REVIEWED | Posted: 23 September 2019 doi:10.20944/preprints201909.0261.v1

et al. [3] also tried to apply the FPS to the main control room of NPP and showed the applicability of the FPS using shaking table test and analytical method. Jeon et al. [4] developed the cone-type friction pendulum bearing system (CFPBS) to prevent the damage of communication equipment during an earthquake, and verify the performance of the CFPBS by numerical analysis and by the shaking table test. However, the FPS shows a difference in performance according to the frictional force, and the frictional force changes depending on the mass of the superstructure. Low frictional forces may require additional dampers to control displacement [2]. Cho et al. [5] performed shaking table test on telecommunication facility using LM guide and spring isolation table and displayed the effect of reducing response acceleration.

Finally, the method of improving the seismic performance using the vibration control device is to install a system consisting of additional mass, damping and stiffness in the structure or the cabinet, and absorb the vibration energy which is generated from the device by the additional mass. This vibration control device was proposed for a single degree of freedom subjected to harmonic vibration by Den Hartog [6]. Warburton [7] proposed the optimum frequency and optimal damping ratio of TMD for random vibration. Since then, many researchers have been conducted as a way to reduce the wind induced vibration of the building [8, 9, 10, 11, and 12].

Recently, some of the researches have been done to reduce the vibration of structures against earthquakes. Domizio et al. [13] showed a vibration reduction effect using TMDs on a four-story steel frame against strong earthquakes. After that, Rahman et al. [14] proposed a method of using part of a wall of a building as the mass of TMD as a method to reduce the vibration of building structures against earthquakes. Then, Salvi et al. [15] studied the effects of soil-structure interaction on low frequency and high frequency multi-story frame structures. In addition, Bagheri and Vahid Rahmani [16] proposed an inelastic tuned mass damper as a way to reduce the seismic response and showed the effect of reducing the seismic response to various structures and earthquakes. Lu et al. [17] proposed an optimal TMD design method to reduce the dynamic displacement of a nonlinear building under unknown earthquake excitations.

Chang et al. [18] proposed the Stockbridge damper as a method to reduce the vibration of the pipe system inside the NPP, and analytically showed the effect of reducing the acceleration of the pipe during earthquakes. Kwag et al. [19] studied the effects of multiple TMD to improve the seismic performance of a nuclear piping system subjected to an earthquake load. However, research on reducing vibration by installing the TMD in a cabinet in an NPP has not been conducted.

In this study, the TMD has been proposed as a way to mitigate the acceleration response of the internal electrical cabinet in NPP. The TMD was designed by the eigenvalue analysis results of the electrical cabinet, and the TMD and the cabinet were modeled using SAP2000 software, a finite element analysis program. The sine sweep wave was used as the input load to confirm the dynamic behavior of the cabinet according to the frequency change and the control effect by the TMD. In order to confirm the control effects of the TMD under earthquakes, the seven recorded earthquakes in Korea and California were used in this investigation. The results manifest that the TMD provides a significant control on the seismic response of cabinet facility under different earthquakes.

2. Numerical Modeling of the Electric Cabinet in NPP

2.1. Description of the Electric Cabinet

NPP consist of many electrical cabinet facilities that vary in size and mass and are used for the power distribution system. In order to confirm the seismic performance of the electrical cabinet inside the NPP, shaking table tests or impact hammer test should be carried out. However, shaking table testing of the cabinet during NPP operation is practically impossible. Therefore, the seismic performance of the internal electrical cabinet of NPP is mainly conducted by the analytical method.

In this study, the cabinet as shown in Figure. 1 was used to confirm the acceleration response of the electrical cabinet inside NPP under earthquakes and was modeled in SAP2000 software. The dimensions of the cabinet are 0.8m×0.8m×2.1m and the total mass is 259kg. The base of the cabinet is

Preprints (www.preprints.org) | NOT PEER-REVIEWED | Posted: 23 September 2019 doi:10.20944/preprints201909.0261.v1

restrained using 8 connection as shown in Figure. 1. Material properties of the cabinet are shown in Table 1.

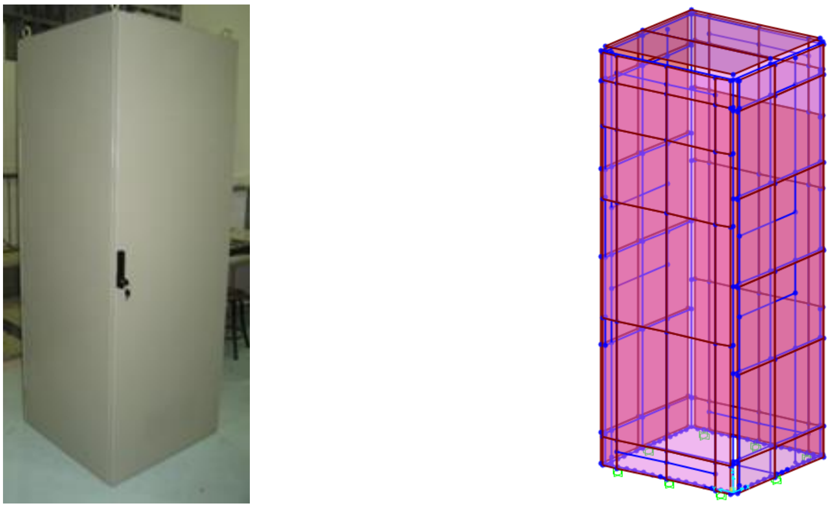

(a) (b)

Figure 1. Model of the electric cabinet: (**a**) Prototype of the cabinet; (**b**) Finite element model

Table 1. Material properties

Item	Value	Unit
Young's modulus	2.14e+5	MPa
Poisson's ratio	0.30	-
Steel density	7,851	kg/m^3

2.2. Eigenvalue Analysis

In order to design a vibration control device to reduce the acceleration of the cabinet, the dynamic properties of the cabinet need to consider. The dynamic properties of the cabinet are obtained using the eigenvalue analysis. One hundred modes were used for the eigenvalue analysis. However, the third mode showed global behavior as shown in Figure 2, while the remaining modes represented the local mode. Therefore, the third mode was selected to be controlled by a vibration control device. The frequency for control mode is 15 Hz and the modal mass is calculated using the following equation.

$$modal\ mass = \sum_{i=1}^{n} m_i \times \delta_{ij}^2 \tag{1}$$

where n is the number of nodes, m_i is a mass of ith node, δ_{ij} is an eigenvector of ith node of jth mode. Structural damping of 5% was assumed for the earthquake analysis. The dynamic properties for the cabinet are shown in Table 2

Table 2. Dynamic properties

	Value	Unit
3rd frequency	15.13	Hz
Modal mass	133	Kg
Structural damping	5.0	%

Preprints (www.preprints.org) | NOT PEER-REVIEWED | Posted: 23 September 2019 doi:10.20944/preprints201909.0261.v1

Figure 2. Dominant global mode of the cabinet

2.3. Design of the Tuned Mass Damper (TMD)

The design variables of the TMD are function of the mass ratio. Warburton [7] proposed the optimum frequency and optimal damping ratio of TMD for random vibration, and are expressed as equation (2) and (3).

$$f_{opt} = \frac{\sqrt{1+\mu/2}}{1+\mu} \tag{2}$$

$$\xi_{opt} = \sqrt{\frac{\mu(1+3\mu/4)}{4(1+\mu)(1+\mu/2)}} \tag{3}$$

where μ is a mass ratio of the TMD, f_{opt} is an optimal frequency ratio, ξ_{opt} is an optimal damping ratio. Table 3 shows the parameters of the designed TMD.

Table 3. Properties of TMD

Parameters	**TMD**	**Unit**
Mass	6	kg
Mass ratio	0.0450	-
Frequency ratio	0.968	-
Stiffness	50,736	N/m
Damping ratio	10.5	%
Damping	115.3	N/m·sec

2.4. Numerical Model

Figure 3(a) shows the electrical cabinet without TMD and Figure 3(b) shows the cabinet with TMD. In Figure 3(b), the green line in a circle represents the TMD. The TMD and cabinet were modeled using SAP2000. Two points link was used for modeling of the TMD in SAP2000. The initial point is attached to the top of the cabinet. And mass of the TMD was added to the end point. Using the TMD design parameters in Table 3, the stiffness of the link (50,736N/m), the damping coefficient (115.3N/m · sec), and the mass (6kg) were applied.

Preprints (www.preprints.org) | NOT PEER-REVIEWED | Posted: 23 September 2019 doi:10.20944/preprints201909.0261.v1

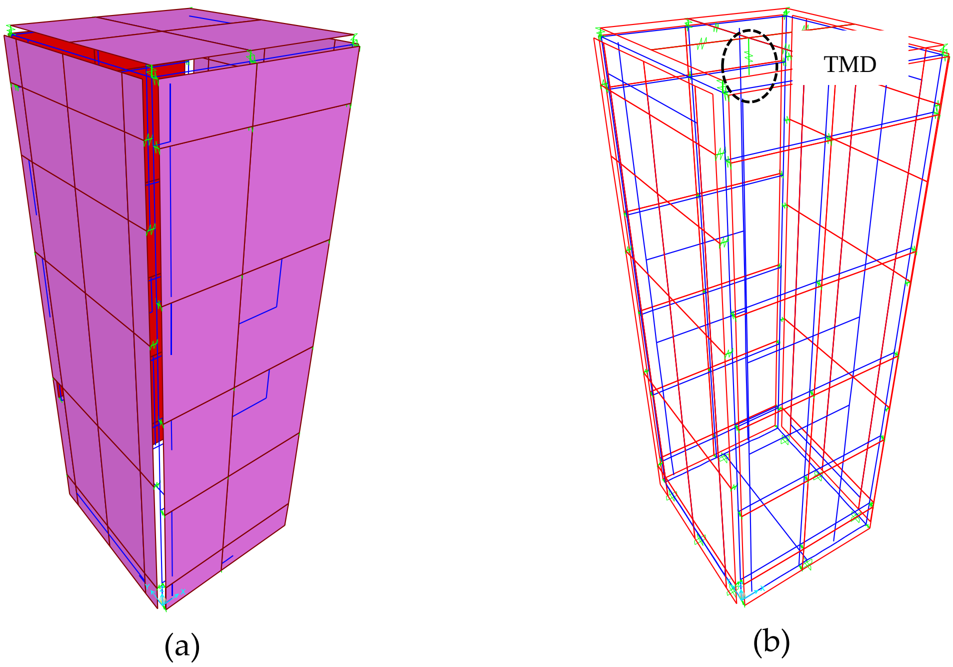

Figure 3. Analytical models without and with controller: (**a**) Electric cabinet without TMD; (**b**) Electric cabinet with TMD

3. Base Excitation

3.1. Sine Sweep Wave

In this study, TMD was applied to reduce the acceleration of the electrical cabinet inside NPP under earthquakes. A sine sweep wave was used to confirm the response properties of the cabinet according to the frequency range of the cabinet and vibration control performance of the TMD. The time history of the sweep wave and its fast Fourier transform (FFT) are showed in Figure 4. The maximum acceleration magnitude of the sine sweep wave is $0.01\mathrm{m}/sec^2$ and the frequency range is 0.1Hz to 250Hz.

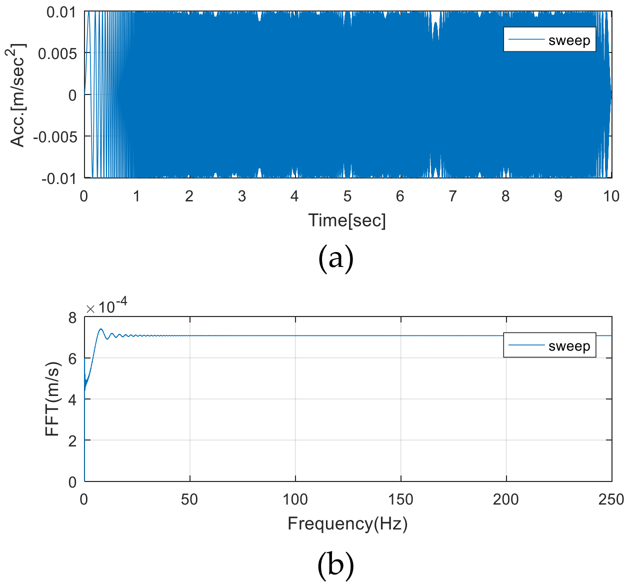

Figure 4. Sine sweep wave and its FFT: (**a**) Sweep wave; (**b**) FFT

3.2. Earthquake Ground Motion

Seven ground motions recorded in Korea were used to confirm the vibration control performance and applicability of TMD. California earthquake was also applied to take into account low frequency. The time history and response spectrum of the earthquakes are shown in Figures 5 to 12, and the characteristics of each earthquake are summarized in Table 4.

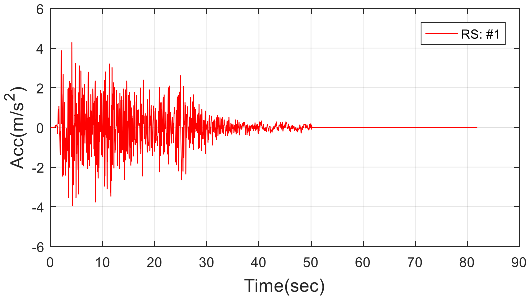

(a)

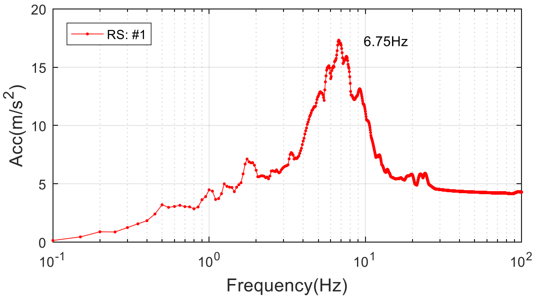

(b)

Figure 5. Earthquake no.1: (**a**) time history; (**b**) response spectrum

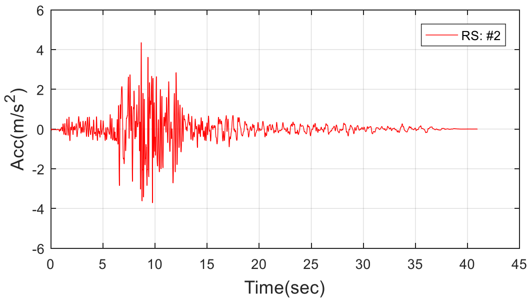

(a)

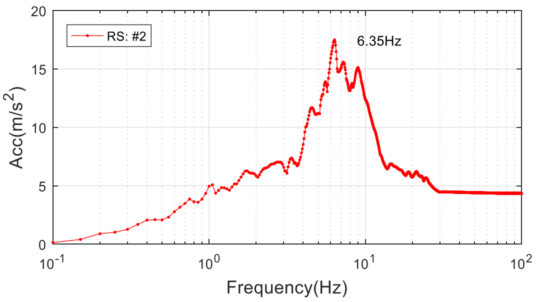

(b)

Figure 6. Earthquake no.2: (**a**) time history; (**b**) response spectrum

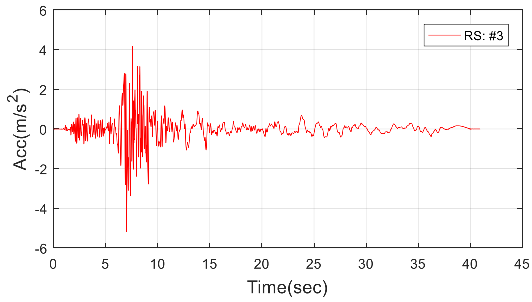

(a)

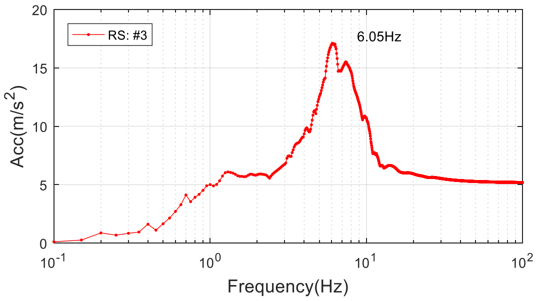

(b)

Figure 7. Earthquake no.3: (**a**) time history; (**b**) response spectrum

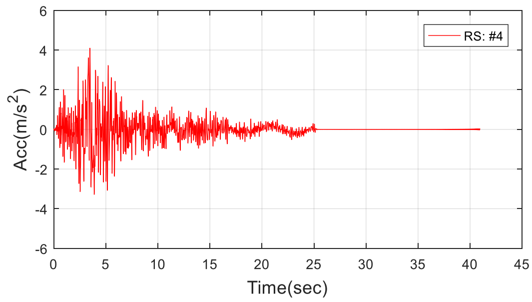

(a)

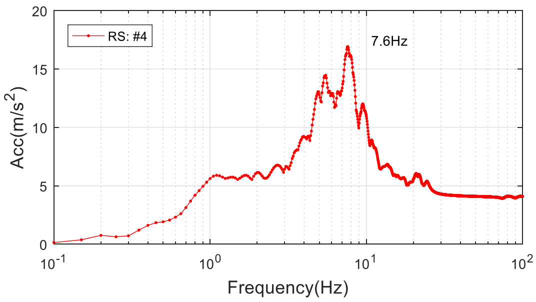

(b)

Figure 8. Earthquake no.4: (**a**) time history; (**b**) response spectrum

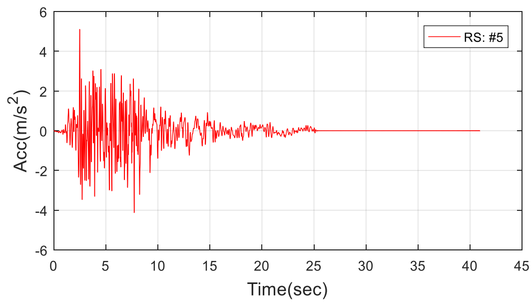

Preprints (www.preprints.org) | NOT PEER-REVIEWED | Posted: 23 September 2019 doi:10.20944/preprints201909.0261.v1

(a)

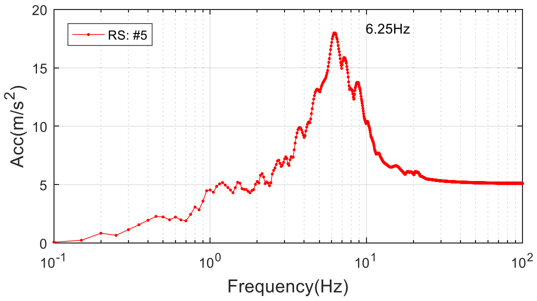

(b)

Figure 9. Earthquake no.5: (**a**) time history; (**b**) response spectrum

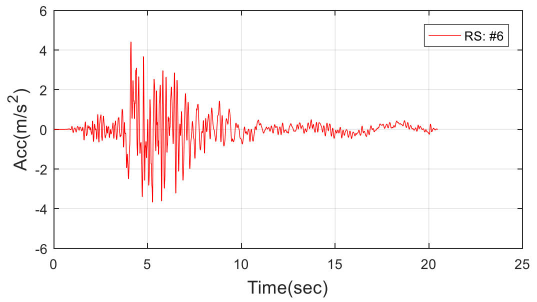

(a)

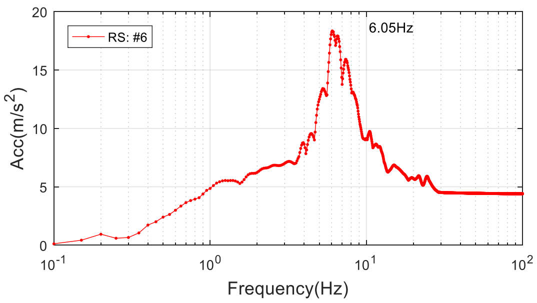

(b)

Figure 10. Earthquake no.6: (**a**) time history; (**b**) response spectrum

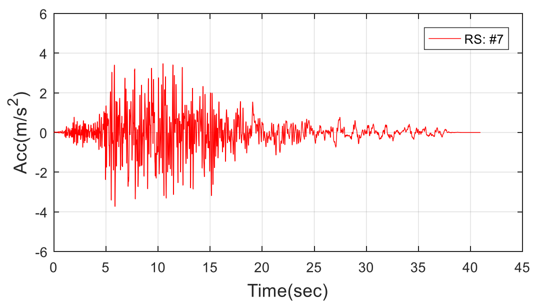

(a)

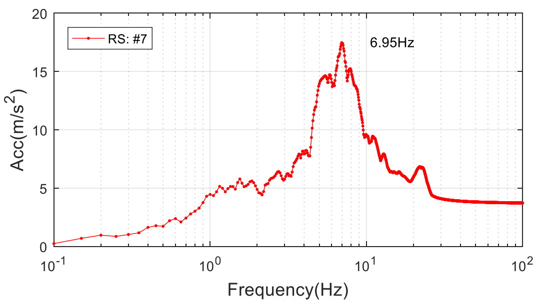

(b)

Figure 11. Earthquake no.7: (**a**) time history; (**b**) response spectrum

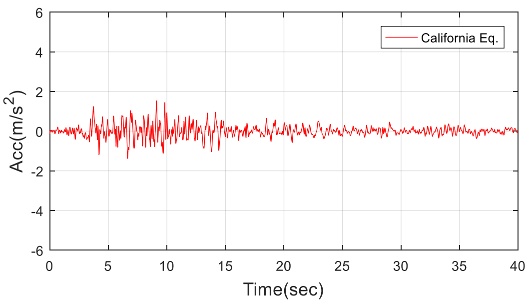

(a)

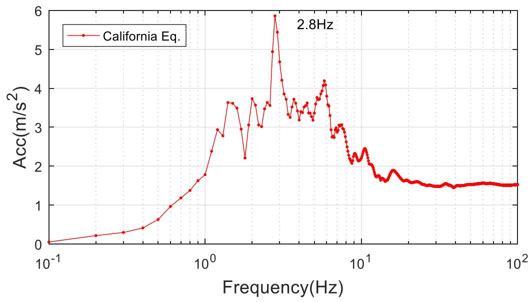

(b)

Figure 12. California earthquake: (**a**) time history; (**b**) response spectrum

Table 4. Characteristic of Earthquakes

Earthquakes	PGA(g)	Sampling time(sec)	Frequency
EQ. 01	0.437	0.010	6.75
EQ. 02	0.443	0.005	6.35
EQ. 03	0.529	0.005	6.05
EQ. 04	0.418	0.010	7.60
EQ. 05	0.521	0.005	6.25
EQ. 06	0.449	0.005	6.05
EQ. 07	0.380	0.005	6.95
California	0.156	0.020	2.80

The recoded ground motions consist the PGA ranges from 0.38 g to 0.529 g and the main frequency range is in the 4 to 9 Hz range. In case of California earthquake, the PGA is 0.156 g, with a wide frequency range from 1 Hz to 10 Hz, with the largest energy at 2.8 Hz.

4. Results and Discussion

4.1. Acceleration Response of electric cabinet

Preprints (www.preprints.org) | NOT PEER-REVIEWED | Posted: 23 September 2019 doi:10.20944/preprints201909.0261.v1

Sine sweep is used for the excitation of the cabinet facility for the following reason.

1. To confirm the frequency characteristic of the cabinet before and after the installation of TMD.

2. To investigate the reduction in the acceleration response.

Figure 13 shows the time history graph and FFT of the acceleration on the top of the cabinet due to the sine sweep wave. The blue dotted line represents the acceleration response of the cabinet without the TMD, and the solid red line represents the acceleration response of the cabinet where the TMD is installed (Figure 13(a)). The acceleration response (uncontrolled) of the cabinet without TMD shows the highest energy at about 15.0 Hz, but the peaks of acceleration response (controlled) of cabinet with TMD were divided into 13.8 Hz and 16.6 Hz, and the acceleration response of the cabinet was reduced.

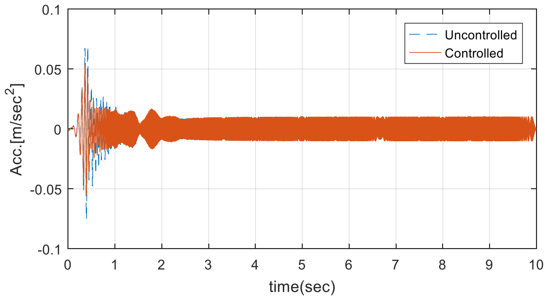

(a)

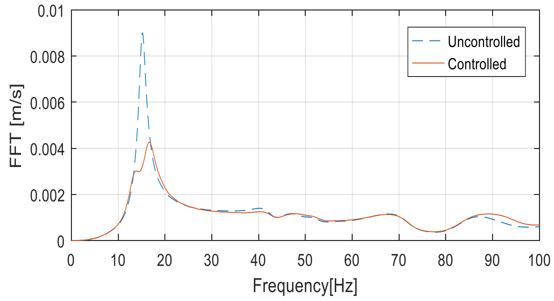

(b)

Figure 13. Acceleration response of cabinet on the top subjected to sine sweep wave: (**a**) time history; (**b**) FFT

4.2. Response of Electric Cabinet Subjected to earthquakes

In Figure 14 (a), the dashed red line shows the acceleration at the top of the cabinet without the TMD, and the blue solid line shows the acceleration response at the top of the cabinet with the TMD. Similarly, in Figure 14 (b), the red line shows the acceleration response spectrum on the top of the cabinet without the TMD, and the blue line shows the acceleration response spectrum on the top of the cabinet after the TMD is installed. In Figure 14 (a), the maximum acceleration response of the cabinet with the TMD under the EQ.01 earthquake is decreased from $4.11\ m/sec^2$ to $3.28\ m/sec^2$, and the decreasing ratio is about 20 %. Root mean square (RMS) of the acceleration is reduced by about 14 %. It can be seen that the response spectrum is significantly reduced between 10 Hz and 20 Hz in Figure 14(b). In the case of EQ. 02 earthquake, the maximum acceleration response was decreased from $4.34\ m/sec^2$ to $3.78\ m/sec^2$, and the decreasing ratio is about 13 % (Figure 15(a)). The maximum acceleration and RMS acceleration results for each earthquake are summarized in Table 5. For the EQ. 06 earthquake, the maximum acceleration was increased by about 3%, but the RMS acceleration is decreased by about 17% (Figure 19). In the case of the California earthquake in Figure 21(a), the maximum acceleration was reduced by about 32% and the response spectrum is decreased by 50% from the peak.

Preprints (www.preprints.org) | NOT PEER-REVIEWED | Posted: 23 September 2019 doi:10.20944/preprints201909.0261.v1

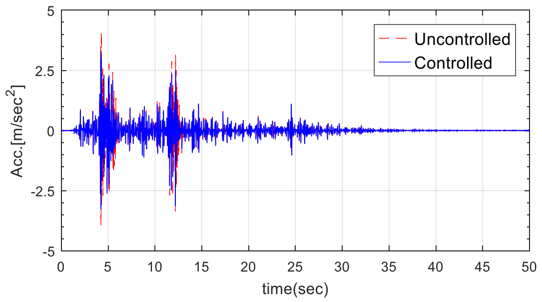

(a)

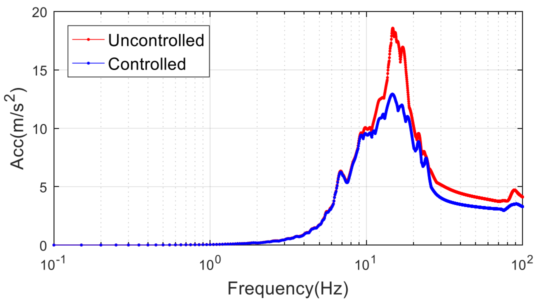

(b)

Figure 14. Response of cabinet subjected to earthquake no.1: (**a**) time history; (**b**) response spectrum

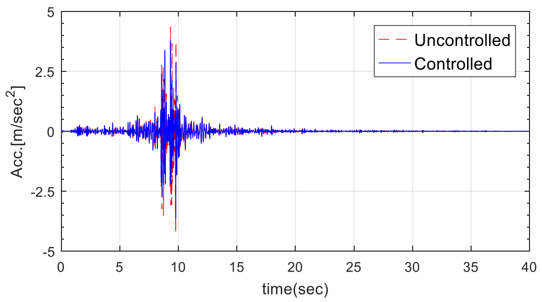

(a)

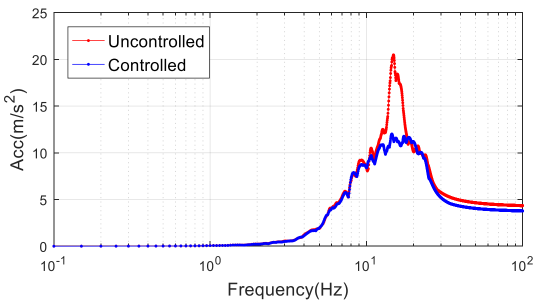

(b)

Figure 15. Response of cabinet subjected to earthquake no.2: (**a**) time history; (**b**) response spectrum

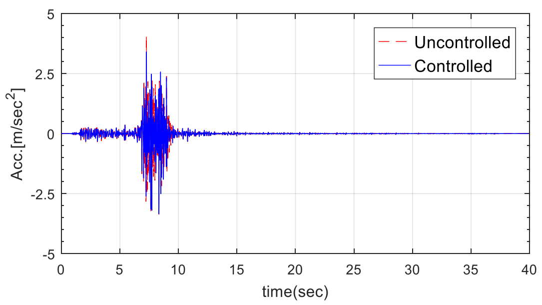

(a)

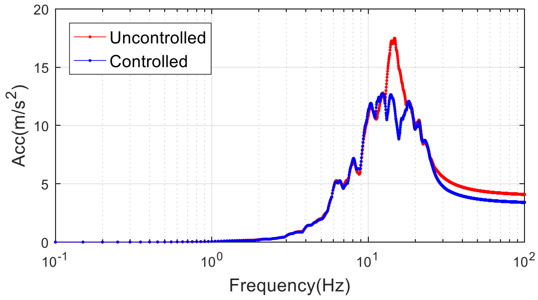

(b)

Figure 16. Response of cabinet subjected to earthquake no.3: (**a**) time history; (**b**) response spectrum

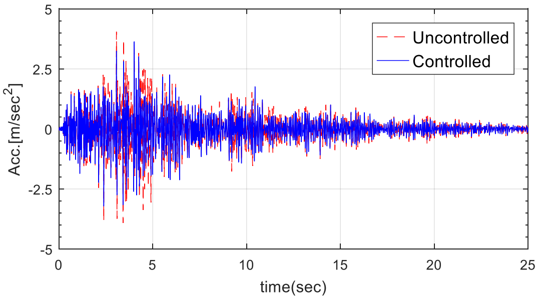

(a)

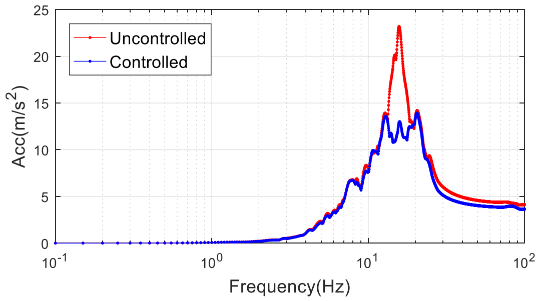

(b)

Figure 17. Response of cabinet subjected to earthquake no.4: (**a**) time history; (**b**) response spectrum

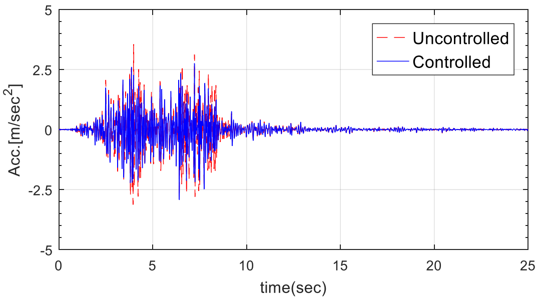

(a)

doi:10.20944/preprints201909.0261.v1

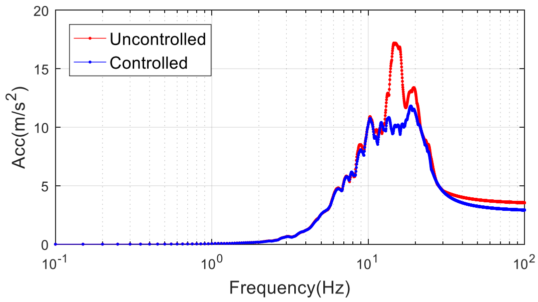

(b)

Figure 18. Response of cabinet subjected to earthquake no.5: (**a**) time history; (**b**) response spectrum

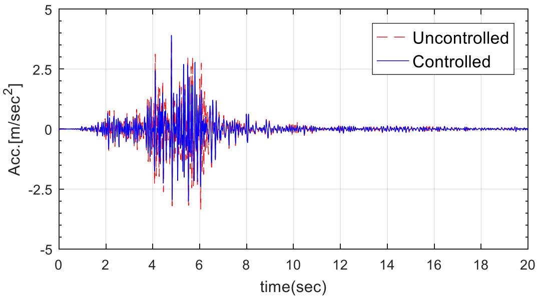

(a)

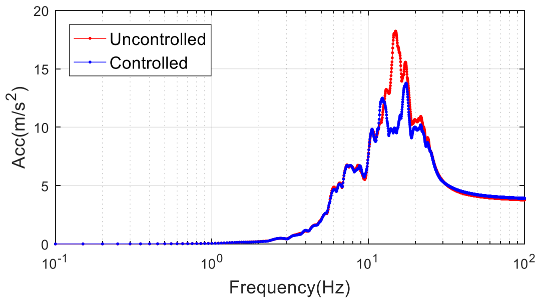

(b)

Figure 19. Response of cabinet subjected to earthquake no.6: (**a**) time history; (**b**) response spectrum

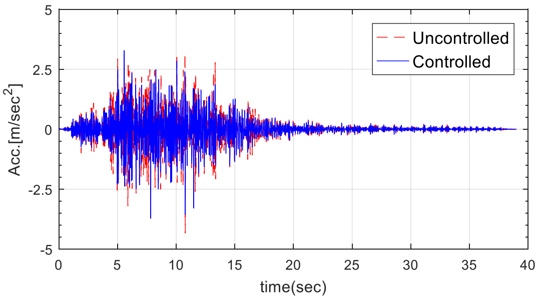

(a)

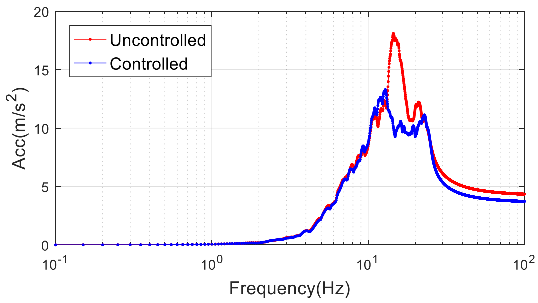

(b)

Figure 20. Response of cabinet subjected to earthquake no.7: (**a**) time history; (**b**) response spectrum

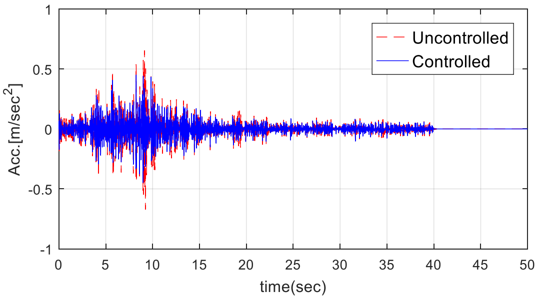

(a)

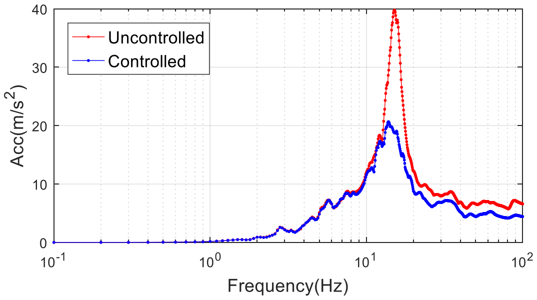

(b)

Figure 21. Response of cabinet subjected to California earthquake: (**a**) time history; (**b**) response spectrum

Direction	Maximum accelaration (m/sec²)			RMS acceleration(m/sec²)		
	Uncontrolled	Controlled	decreasing ratio(%)	Uncontrolled	Controlled	decreasing ratio(%)
EQ. 01	4.11	3.28	20.23	0.38	0.32	14.59
EQ. 02	4.34	3.78	12.96	0.31	0.25	18.34
EQ. 03	4.09	3.41	16.69	0.31	0.27	12.51
EQ. 04	4.04	3.63	10.18	0.66	0.55	17.34
EQ. 05	3.55	2.92	17.68	0.52	0.43	16.88
EQ. 06	3.79	3.91	-3.16	0.48	0.40	17.41
EQ. 07	4.34	3.72	14.29	0.56	0.48	15.23
California	0.67	0.45	32.86	0.08	0.06	22.62

In the results of the dynamic analysis of the electrical cabinet, the acceleration response of the cabinet for the sine sweep wave, the low-frequency earthquake (California earthquake) and the high-frequency earthquake (seven ground motions) were compared. At most dynamic loads, it was found that the acceleration response of the cabinet with TMD was reduced. It has been shown that the proposed TMD can be sufficiently applied as a device to reduce the acceleration response of the cabinet to earthquakes.

5. Conclusions

In this study, TMD was proposed as a method to mitigate the acceleration response of the electrical cabinet inside NPP. A sine sweep wave, seven recorded earthquakes, and the California earthquake were used to simulate the control effects of the response of the cabinet under earthquakes.

The acceleration response before and after the control of the cabinet using the TMD was compared using the time domain and the frequency domain.

The results of the sine sweep wave confirmed that the electrical cabinet is mainly dominated by the first global mode, and the TMD can reduce the acceleration response of the cabinet. It is also confirmed that the TMD can be sufficiently applied to the cabinets inside a nuclear power plant under earthquakes. Therefore, this study analytically proves that TMD could be considered as a method for improving the seismic performance of cabinets.

Further research on the experimental verification of the cabinet with TMD and the evaluation of seismic performance are considered necessary.

References

1. McFarlane, John P. The Seismic Assessment of British Energy's Nuclear Power Stations and Some Pragmatic Solutions to Seismic Modifications. Proceedings of the workshop on the seismic re-evaluation of all nuclear facilities, Ispra, Italy, 26-27 March, 2001.
2. Kim, D.K.; Kim, W.B.; Suh, Y.P.; Moon, D.S.; Kim, J.Y. Seismic Performance Evaluation for MCR of Nuclear Power Plant Isolated by FPS, Proceeding of Earthquake Engineering Society of Korea Conference, 2003, 453-460.
3. Kim, W.B.; Lee, K.; Kim, G.H. Application of friction pendulum system to the main control room of a nuclear power plant, Can. J. Civ. Eng., **2009**, 36, 63-72.
4. Jeon, B.G.; Chang, S.J.; Kim, S.W.; Kim, N.S. Base isolation performance of a cone-type friction pendulum bearing system, Struct. Eng. Mech., **2015**, 53, 227-248.
5. Cho, S.G.; Hwang, K.T.; Park, W.K.; So, G.H. Vibration Response Reduction Effects of Isolation Table System with LM Guide, Proceeding of Earthquake Engineering Society of Korea Conference, 2013, 131-134.
6. Den Hartog, J.P. Mechanical Vibrations, 4th ed.; McGraw-Hill: New York, NY, USA, 1956.
7. Warburton, G.B. Optimum Absorber Parameters for Various Combinations of Response and Excitation Parameters, Earthq. Eng. Struct. D., **1982**, 10, 381-401.
8. Kwok, K.C.S.; Samali, B. Performance of tuned mass dampers under wind loads, Eng. Struct., **1995**, 17, 655-667.
9. Elias, S.; Matsagar, V. Distributed multiple tuned mass dampers for wind vibration response control of high-rise building, J. Eng., **2014**, 2014, 1-11.
10. Elias, S.; Matsagar, V. Research developments in vibration control of structures using passive tuned mass dampers, Annu. Rev. Control, **2017**, 44, 129-156.
11. Giaralis, A.; Petrini, F. Optimum design of the tuned mass-damper-inerter for serviceability limit state performance in wind-excited tall buildings, Procedia Eng., **2017**, 199, 1773-1778.
12. Elias, S.; Matsagar, V. Wind response control of tall buildings with a tuned mass damper, J. Build. Eng., **2018**, 15, 51-60.
13. Domizio, M.; Ambrosini, D. Oscar Curadelli, Performance of tuned mass damper against structural collapse due to near fault earthquakes, J. Sound Vib., **2015**, 336, 32-45.
14. Rahman, M.S.; Chang, S.; Kim, D. Multiple wall dampers for multi-mode vibration control of building structures under earthquake excitation, Struct. Eng. Mech., **2017**, 63, 537-549.
15. Salvi, J.; Pioldi, F.; Rizzi, E. Optimum Tuned Mass Dampers under seismic Soil-Structure Interaction, Soil Dyn. Earthq. Eng., **2018**, 114, 576-597.
16. Bagheri, S.; Vahid Rahmani, D., Seismic response control with inelastic tuned mass dampers, Eng. Struct., 2018, 172, 712-722.
17. Lu, Z.; Li, K.; Ouyang, Y.; Shan, J. Performance-based optimal design of tuned impact damper for seismically excited nonlinear building, Eng. Struct., 2018, 160, 314-327.
18. Chang, S.; Sun, W.; Cho, S.G.; Kim, D. Vibration Control of Nuclear Power Plant Piping System Using Stockbridge Damper under Earthquakes, Sci. Technol. Nucl. Ins., 2016, 2016, 1-12.
19. Kwag, S.; Kwak, J.; Lee, H.; Oh, J.; Koo, G.H. Enhancement in the Seismic Performance of a Nuclear Piping System using Multiple Tuned Mass Dampers, Energies, 2019, 12, 1-26.